Journal of Sound and Vibration (2000) **234**(3), 537–546
doi:10.1006/jsvi.1999.2849, available online at http://www.idealibrary.com on IDEAL®

LETTERS TO THE EDITOR

VIBRATION CONTROL OF A SEMI-ACTIVE SUSPENSION FEATURING ELECTRORHEOLOGICAL FLUID DAMPERS

SEUNG-BOK CHOI AND WAN-KEE KIM

Smart Structures and Systems Laboratory, Department of Mechanical Engineering, Inha University, Incheon 402-751, *Korea*

(*Received* 2 *September* 1999, *and in final form* 26 *November* 1999)

1. INTRODUCTION

Recently, very attractive and effective semi-active suspension featuring electro-rheological fluid dampers (ER dampers in short) has been proposed by many investigators for vibration control of a vehicle system. Petek [1] proposed a cylindrical (mono-tube) ER damper and applied it to the rear suspension of a passenger vehicle for better driving performance over road and bump profiles. Nakano [2] constructed a quarter-car suspension system model installed with cylindrical ER dampers, and demonstrated its effectiveness of the vibration isolation from excitations. Kamath *et al.* [3] proposed an analytical model for the prediction of field-dependent damping forces of a cylindrical ER damper. Gordaninejad *et al.* [4] experimentally evaluated the performance of cylindrical, multi-electrode ER dampers under forced vibration. More recently, Choi *et al.* [5] proposed a cylindrical ER damper and demonstrated its damping force controllability by using a skyhook controller.

As evident from these previous studies, ER dampers proposed so far are cylindrical types consisting of a flow duct between inner and outer electrodes. This type of ER damper has a simple mechanism and hence one can easily analyze field-dependent damping forces. However, in order to achieve an acceptable damping force required for a passenger vehicle an advanced ER fluid, which has relatively high-field-dependent yield stress (about 2·5 kPa at 5 kV/mm), needs to be used for the cylindrical ER damper. Currently, there exist a couple of commercially available ER fluids, which can produce the demanded damping forces. But, those ER fluids are very expensive. Consequently, it is necessary to devise a new type of ER damper whose damping force is much less sensitive to the yield stress of ER fluid.

This work presents a novel type of ER damper and applies it to a semi-active suspension of a passenger vehicle in order to achieve effective vibration control. The proposed ER damper has flow orifices controlled by the intensity of electric field as well as piston motion (orifice-type ER damper in short). Thus, the damping force of the proposed ER damper is less sensitive to the field-dependent yield stress of ER fluid than that of a cylindrical ER damper. After manufacturing the orifice type of ER damper on the basis of a theoretical model, field-dependent damping forces are evaluated. The proposed ER damper is then incorporated with a full-car model in order to evaluate suspension performance. Vibration control responses of the semi-active suspension system under bump and random road profiles are investigated by employing an optimal controller.

2. ORIFICE-TYPE ER DAMPER

The schematic configuration and photograph of the orifice-type ER damper proposed in this work are shown in Figure 1. The moving piston head consists of a main-orifice,

0022-460X/00/280537 + 10 $35.00/0

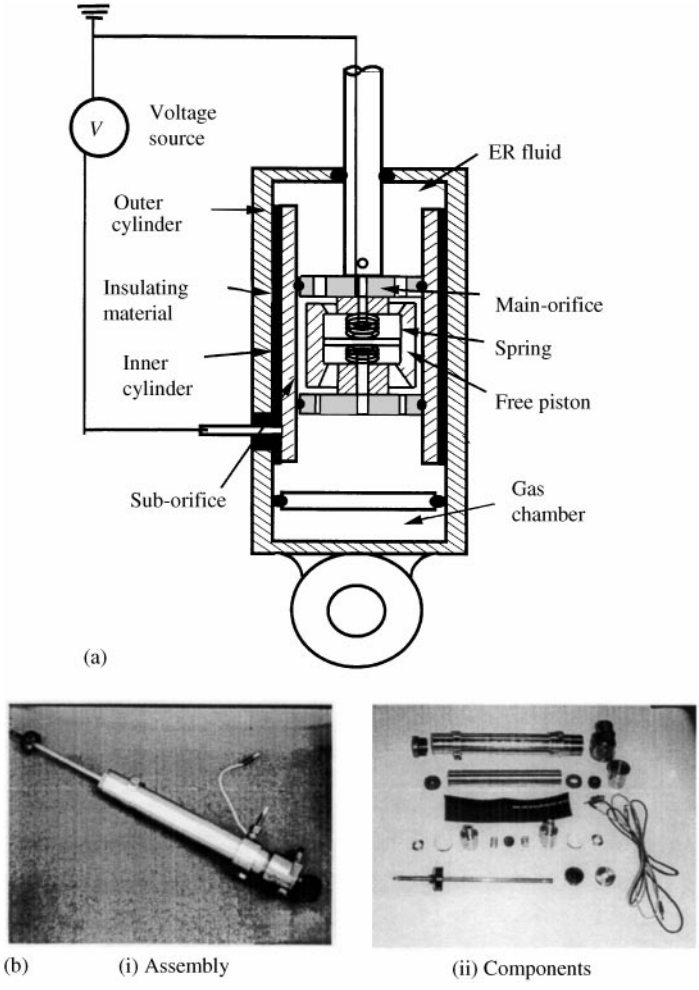

Figure 1. The proposed orifice-type ER damper. (a) Configuration; (b) photograph.

sub-orifices, and a free piston supported by a spring. By the motion of the piston head, the ER fluid flows through the main-orifice and sub-orifices from one damper to the other. The positive voltage is produced by a high-voltage supply unit connected to the inner cylinder, while the negative (ground) voltage is connected to the piston head. On the other hand, the gas chamber located below the lower chamber acts as an accumulator of the ER fluid induced by the motion of the piston. In the absence of electric fields, the flow motion of the ER fluid occurs through the main-orifice and sub-orifices without any geometric change. However, if a certain level of the electric field is applied to the ER damper, the flow motion of the sub-orifices is resisted by the field-dependent yield stress of the ER fluid. This causes the free piston to move up (or down), and hence the flow area of the main-orifice is changed by the intensity of the electric field as well as the piston motion. Therefore, we can achieve controllable damping forces not only from the yield stress of the ER fluid, but also from the fluid resistance due to the controllable geometric change. This is a salient difference from the cylindrical ER damper, in which controllable damping force depends on only the yield stress of the ER fluid.

The damping force (F) of the proposed ER damper can be expressed by

$$F = \frac{A_r^2}{C_g} x + (P_{ER} + R_e Q + \rho_{ER} g(h_f + h_r))(A_p - A_r - A_o). \tag{1}$$

In the above equation A_p, A_r and A_o are the sectional areas of piston, piston rod and orifice respectively. C_g is the gas compliance, x is the moving distance of the piston rod, ρ_{ER} is the density of the ER fluid, g is the gravitational acceleration, Q is the flow rate passing through the orifices, and h_f and h_r are the head loss in orifices. The flow resistance R_e due to the viscosity, and pressure drop P_{ER} due to the field-dependent yield stress are given by

$$R_e = \frac{12\eta L}{bh^3}, \qquad P_{ER} = 2\frac{L}{h}\alpha E^{\beta}, \tag{2}$$

where η is the viscosity of the ER fluid, L is the electrode length of the inner cylinder, b is the electrode width, h is electrode gap between inner and outer cylinders, E is the electric field applied to the ER fluid damper, α and β are experimentally determined constants characterizing the yield stress of the ER fluid. It is noted from equation (1) that the first term represents the damping force due to the gas compliance, the second from the field-dependent yield stress of the ER fluid, the third for the flow resistance due to viscosity, and the fourth due to the head loss of the orifices.

On the basis of the damper model (1), field-dependent damping forces are analyzed. The following principal design parameters are determined in view of a small-sized passenger vehicle: electrode length = 70 mm, electrode gap = 0·75 mm, piston head diameter = 35 mm, main orifice diameter = 8 mm, and suborifice diameter = 2·5 mm. Figure 2 presents the predicted and measured damping forces with respect to the piston velocity. In this study, arabic gum and transformer oil are chosen as particles and base liquid respectively. The particle concentration of the ER fluid is 35% by weight. The yield stress of the employed ER fluid is experimentally obtained by 1·4 kPa at 5 kV/mm. This is relatively a low value compared with commercially available ER fluids, which exhibit about 2·5 kPa at 5 kV/mm. It is observed from Figure 2 that the agreement between the predicted and measured results is good. This directly validates the damper model given by equation (1). It is also observed from Figure 2 that unlike the cylindrical ER damper [1,5], the damping force drastically increases at a certain piston velocity in the presence of 3·0 kV/mm. This, of course is, due to the geometric change of the orifices. Figure 3 presents the measured damping force at various electric fields. We see that the damping force is increased up to 1100 N by applying the electric field of 5 kV/mm. This level of the damping force is enough to take into account the suspension system of a small-sized passenger vehicle. It is also noted from Figure 3 that the positive damping force (rebound motion of the piston) is much larger than the negative damping force (jounce motion). This damping force specification is normally required for practical application of a vehicle suspension system. In this work, the stiffness constant of the spring, which supports the free piston, is adjusted to obtain the different damping force between rebound and jounce motions. It is remarked that the detailed experimental procedures to measure the field-dependent damping forces are well described in reference [5].

3. SEMI-ACTIVE SUSPENSION SYSTEM

The proposed orifice-type ER damper is then applied to a full-car suspension model in order to evaluate the effectiveness of vibration isolation as shown in Figure 4. The vehicle

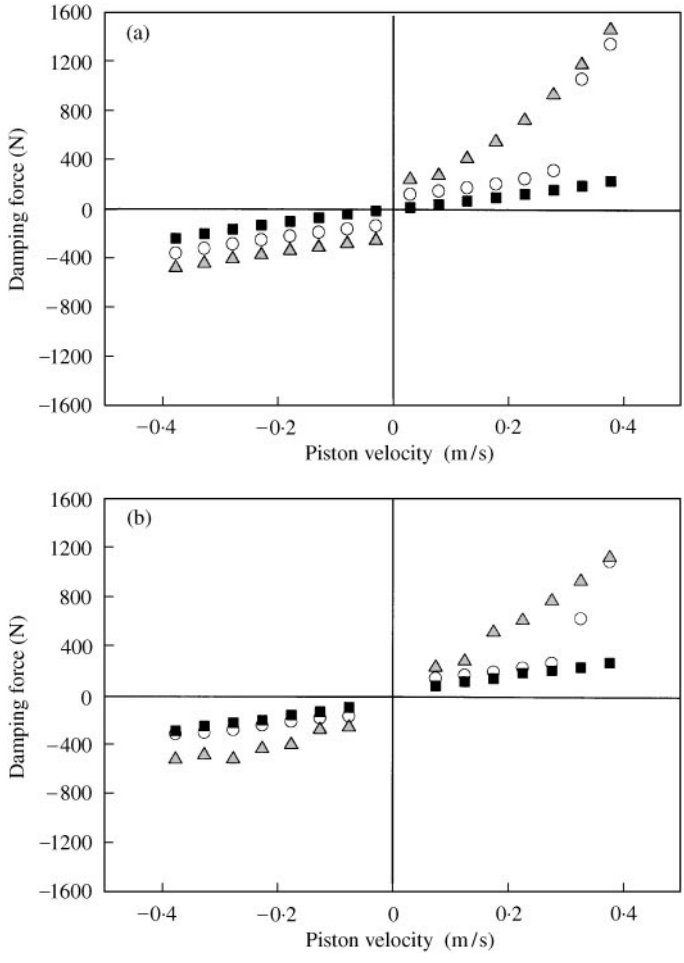

Figure 2. Damping force versus piston velocity. (a) Predicted; ■, 0·0 kV/mm; ○, 3·0 kV/mm; △, 5·0 kV/mm; (b) measured.

body itself is assumed to be rigid and has degree of freedom (d.o.f.) in the vertical, pitch and roll directions. It is connected to four rigid bodies representing wheel unsprung masses in which each has a vertical d.o.f. From the dynamic model, the governing equations of motion are derived as follows:

$$
\begin{aligned}
M\ddot{z}_g &= -f_{s1} - f_{s2} - f_{s3} - f_{s4} + F_{ER1} + F_{ER2} + F_{ER3} + F_{ER4},\\
J_\theta\ddot{\theta} &= af_{s1} + af_{s2} - bf_{s3} - bf_{s4} - aF_{ER1} - aF_{ER2} + bF_{ER3} + bF_{ER4},\\
J_\phi\ddot{\phi} &= -cf_{s1} + df_{s2} - cf_{s3} + df_{s4} + cF_{ER1} - dF_{ER2} + cF_{ER3} - dF_{ER4},\\
m_1\ddot{z}_{us1} &= f_{s1} - f_{t1} - F_{ER1}, \qquad m_2\ddot{z}_{us2} = f_{s2} - f_{t2} - F_{ER2},\\
m_3\ddot{z}_{us3} &= f_{s3} - f_{t3} - F_{ER3}, \qquad m_4\ddot{z}_{us4} = f_{s4} - f_{t4} - F_{ER4}.
\end{aligned}
\tag{3}
$$

Here, F_{ERi}, is controllable damping force of the proposed orifice ER damper, $f_{si} = k_{si}(z_{si} - z_{usi}) + c_{si}(\dot{z}_{si} - \dot{z}_{usi})$, and $f_{ti} = k_{ti}(z_{usi} - z_i)$ for $i = 1, 2, 3, 4$. In addition, M is the

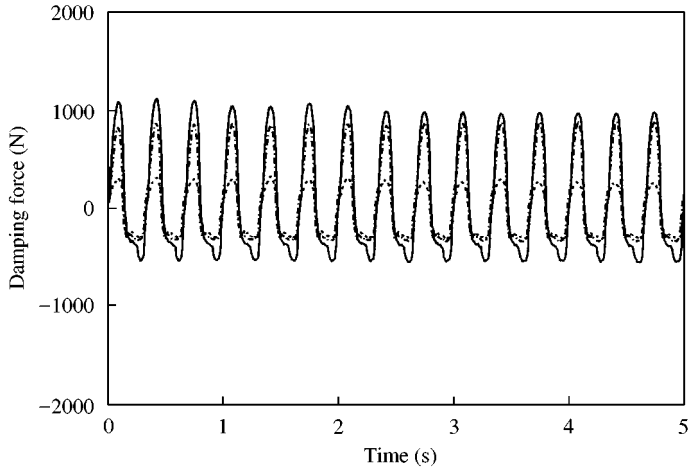

Figure 3. Time history of the measured damping forces: ----------, 0·0 kV/mm; -·-·-·-·-, 3·0 kV/mm; ——, 5·0 kV/mm.

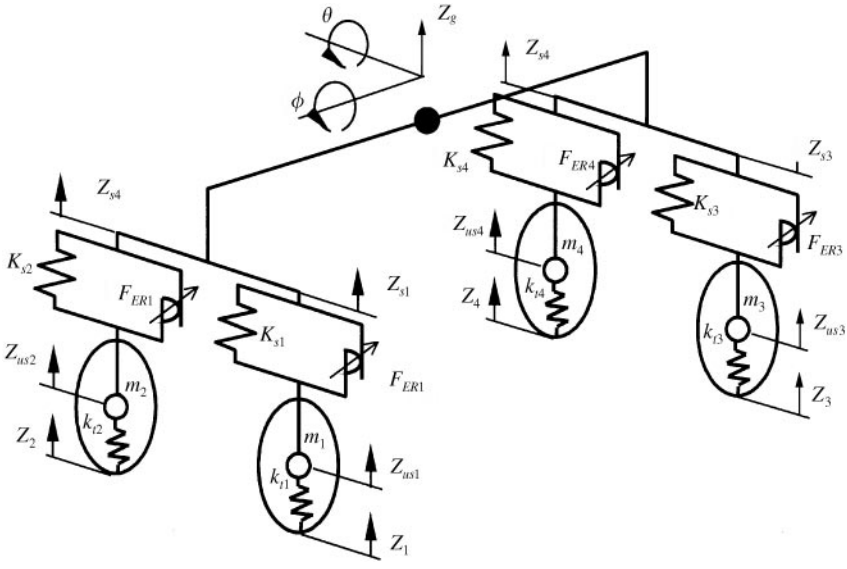

Figure 4. Dynamic model of a vehicle suspension featuring the orifice-type ER dampers.

sprung mass and $m_i (i = 1, 2, 3, 4)$ is the unsprung mass. J_θ and J_ϕ are the pitch and roll mass moment of inertia respectively. $k_{si} (i = 1, 2, 3, 4)$ is total stiffness coefficient of the suspension, and $c_{si} (i = 1, 2, 3, 4)$ is damping coefficient of the suspension. $k_{ti} (i = 1, 2, 3, 4)$ is stiffness coefficient of the tire. z_g, z_{usi} and $z_i (i = 1, 2, 3, 4)$ are the verticle displacement of sprung mass, unsprung mass and excitation respectively. θ and ϕ are the pitch and roll angular displacement. a, b, c and d are the distance between the front damper and center of gravity (CG) of the sprung mass, the distance between the rear and CG, the distance between the left and CG, and the distance between the right and CG respectively. Now, in order to formulate optimal controller for vibration suppression, the dynamic model (3) can be

expressed in a state-space form as

$$\dot{\mathbf{x}} = \mathbf{A}\mathbf{x} + \mathbf{B}\mathbf{u} + \mathbf{D}\mathbf{w}, \tag{4}$$

where

$$\mathbf{x} = [x_1, x_2, x_3, x_4, x_5, x_6, x_7, x_8, x_9, x_{10}, x_{11}, x_{12}, x_{13}, x_{14}]^{\mathrm{T}} = [z_g, \dot{z}_g, \theta, \dot{\theta}, \phi, \dot{\phi}, z_{us1}, \dot{z}_{us1}, z_{us2}, \dot{z}_{us2}, z_{us3}, \dot{z}_{us3}, z_{us4}, \dot{z}_{us4}]^{\mathrm{T}},$$

$$\mathbf{u} = [u_1, u_2, u_3, u_4]^{\mathrm{T}} = [F_{ER1}, F_{ER2}, F_{ER3}, F_{ER4}]^{\mathrm{T}},$$

$$\mathbf{w} = [w_1, w_2, w_3, w_4]^{\mathrm{T}} = [z_1, z_2, z_3, z_4]^{\mathrm{T}}.$$

In the above, $\mathbf{A} \in \Re^{14\times 14}$, $\mathbf{B} \in \Re^{14\times 4}$ and $\mathbf{D} \in \Re^{14\times 4}$ are the system matrix, the control input matrix, and the disturbance matrix, respectively. On the other hand, in practical situation, we normally use accelerometers to measure vertical motions such as z_{usi} and $\dot{z}_{usi}$. Therefore, from the defined state variables, the output equation can be formulated as

$$\mathbf{y} = \mathbf{C}\mathbf{x}, \tag{5}$$

where $\mathbf{C} \in \Re^{1\times 14}$ is the system output matrix. Since the state variables θ and ϕ are not available from direct measurement, a state observer needs to be used to estimate the variables which are eventually incorporated with state feedback optimal controller.

In this work, we adopt conventional optimal controller, which is frequently employed to suspension system of vehicles. The performance index to be minimized is given by

$$\mathbf{J} = \int_0^\infty \{\mathbf{x}^{\mathrm{T}}\mathbf{Q}\mathbf{x} + \mathbf{u}^{\mathrm{T}}\mathbf{R}\mathbf{u}\}\,\mathrm{d}t, \tag{6}$$

where $\mathbf{Q}$ is the state weighting semi-positive matrix, and $\mathbf{R}$ is the input weighting positive matrix. Since the suspension system ($\mathbf{A}$, $\mathbf{B}$) in equation (4) is controllable, we can obtain the following state feedback controller.

$$\mathbf{u} = -\mathbf{K}\mathbf{x}, \qquad \mathbf{K} = \mathbf{R}^{-1}\mathbf{B}^{\mathrm{T}}\mathbf{P}. \tag{7}$$

In the above, $\mathbf{K}$ is state feedback gain matrix, and $\mathbf{P}$ is the solution of the following algebraic Riccati equation:

$$\mathbf{A}^{\mathrm{T}}\mathbf{P} + \mathbf{P}\mathbf{A} - \mathbf{P}\mathbf{B}\mathbf{R}^{-1}\mathbf{B}^{\mathrm{T}}\mathbf{P} + \mathbf{Q} = \mathbf{0}. \tag{8}$$

As mentioned earlier, *all of the state variables*, $\mathbf{x}$ are not available from direct sensor measurment. Thus, from the observability of the system ($\mathbf{A}$, $\mathbf{C}$), we construct the following full order state observer:

$$\dot{\hat{\mathbf{x}}} = \mathbf{A}\hat{\mathbf{x}} + \mathbf{B}\mathbf{u} + \mathbf{L}(\mathbf{y} - \mathbf{C}\hat{\mathbf{x}}), \qquad \mathbf{L} = \mathbf{P}_1\mathbf{C}^{\mathrm{T}}\mathbf{R}_1^{-1}, \tag{9}$$

where $\hat{\mathbf{x}}$ are the estimated state variables, $\mathbf{L}$ is the observer gain matrix, and $\mathbf{P}_1$ is obtained from the following Riccati equation:

$$\dot{\mathbf{P}}_1 = \mathbf{A}\mathbf{P}_1 + \mathbf{P}_1\mathbf{A}^{\mathrm{T}} - \mathbf{P}\mathbf{C}^{\mathrm{T}}\mathbf{R}_1^{-1}\mathbf{C}\mathbf{P}_1 + \mathbf{Q}_1, \tag{10}$$

where $\mathbf{Q}_1$ is the positive-semi-definite matrix, and $\mathbf{R}_1$ is the positive-definite matrix. It is noted that once the observer dynamics (9) is incorporated with the feedback control

dynamics (4) and (7), the state error between actual and estimated ones becomes zero for arbitrary initial conditions.

On the other hand, it is known that the proposed ER damper is a semi-active actuator. Thus, the control input force should be applied to the ER suspension system according to the following actuating condition.

$$u_1 = \begin{cases} u_l & \text{for } u_i(\dot{z}_{usi} - \dot{z}_{si}) > 0 \\ 0 & \text{for } u_i(\dot{z}_{usi} - \dot{z}_{si}) \leqslant 0 \end{cases} \quad (i = 1, 2, 3, 4). \tag{11}$$

This condition physically implies that the actuating of the controller u_i only assures the increment of energy dissipation of the stable system.

4. VIBRATION CONTROL RESPONSES

The system parameters of the semi-active suspension system are chosen on the basis of conventional suspension system of a small-sized passenger vehicle, and those values are as follows: $M = 1000$ kg.

$$m_1 = m_2 = 29{\cdot}5 \text{ kg}, \qquad m_3 = m_4 = 27{\cdot}5 \text{ kg}, \qquad J_\theta = 1356 \text{ kg m}^2,$$

$$J_\phi = 480 \text{ kg m}^2, \qquad k_{s1} = k_{s2} = 20\,580 \text{ N/m},$$

$$k_{s3} = k_{s4} = 19\,600 \text{ N/m}, \qquad k_{t1} = k_{t2} = k_{t3} = k_{t4} = 200\,000 \text{ N/m},$$

$$a = 0{\cdot}96 \text{ m}, \; b = 1{\cdot}44 \text{ m}, \qquad c = d = 0{\cdot}71 \text{ m}.$$

Prior to investigating vibration control performance, the effectiveness of the stable observer is verified. Figure 5 presents state estimations of vertical displacement and pitch angular displacement at CG. It is clearly observed the the estimated state tracks well to the real one in a very short time validating the applicability of all state variables to the feedback controllers.

Control characteristics for vibration suppression of the full-car ER suspension system are evaluated under two types of road excitations. The first excitation, normally used to reveal the transient response characteristic, is a bump described by

$$\begin{aligned} z_i &= z_b[1 - \cos(w_r t)] \quad \text{for } i = 1, 2, \\ \mathrm{z}_i &= \mathrm{z}_b[1 - \cos(w_r(t - D_{car}/V))] \quad \text{for } j = 3, 4. \end{aligned} \tag{12}$$

Here, $w_r = 2\pi V/D$, z_b($= 0{\cdot}035$ m) is the half of the bump height. D ($= 0{\cdot}8$ m) is the width of the bump, D_{car} ($= 2{\cdot}4$ m) is the wheel base which is defined as the distance between the front wheel and the rear one, and V is the vehicle velocity. In the bump excitation, the vehicle travels the bump with constant velocity of 3·08 km/h ($= 0{\cdot}856$ m/s). Figure 6 presents time responses at CG of the proposed semi-active suspension system for the bump excitation. It is clearly seen that both vertical acceleration and pitch angular acceleration are substantially reduced by employing the optimal controller. The improvement of these suspension characteristics is directly related to the improvment of the ride comfort of the vehicle.

The second type of road excitation, normally used to evaluate frequency response, is a stationary random process with zero mean described by

$$\dot{Z}_i + \rho V Z_i = V W_{ni} \quad (i = 1, 2, 3, 4). \tag{13}$$

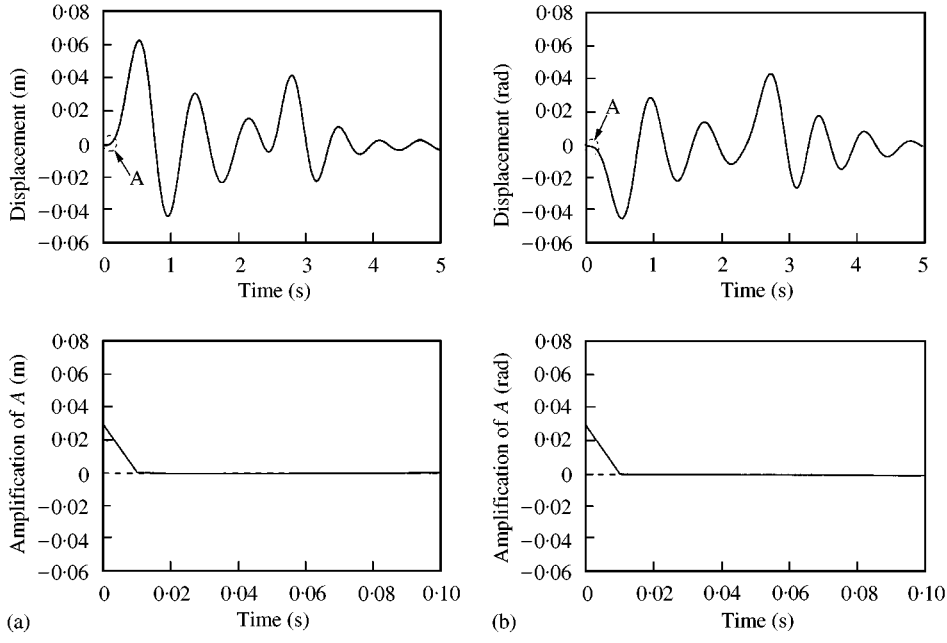

Figure 5. Performance of the full order state observer. (a) Vertical displacement; (b) pitch angular displacement: ----, actual; ——, estimated.

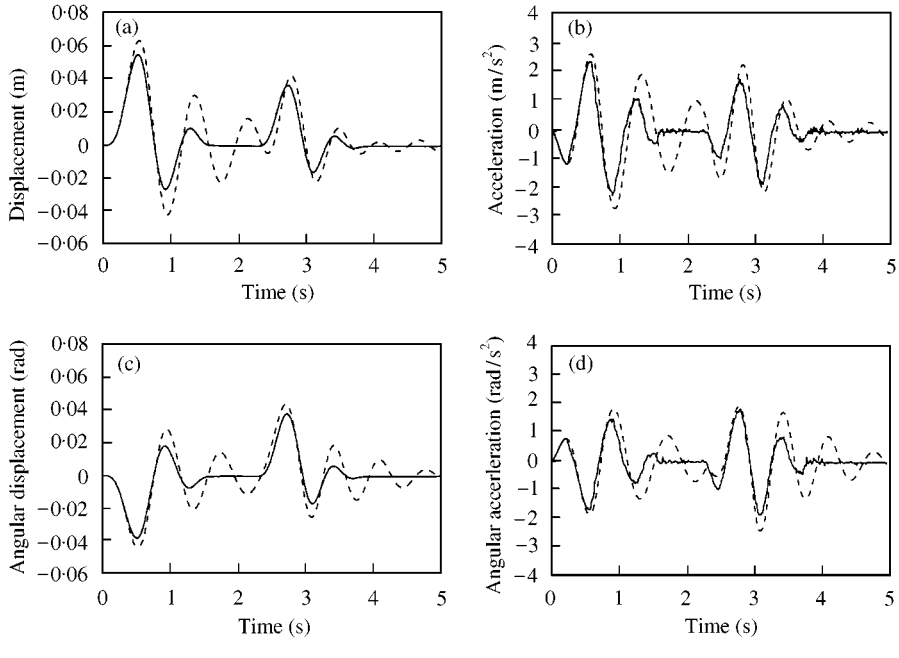

Figure 6. Bump responses of the semi-active suspension with the orifice-type ER dampers. (a) Vertical displacement; (b) vertical acceleration; (c) pitch angular displacement; (d) pitch angular acceleration: ---, 0·0 kV/mm; ——, optimal control.

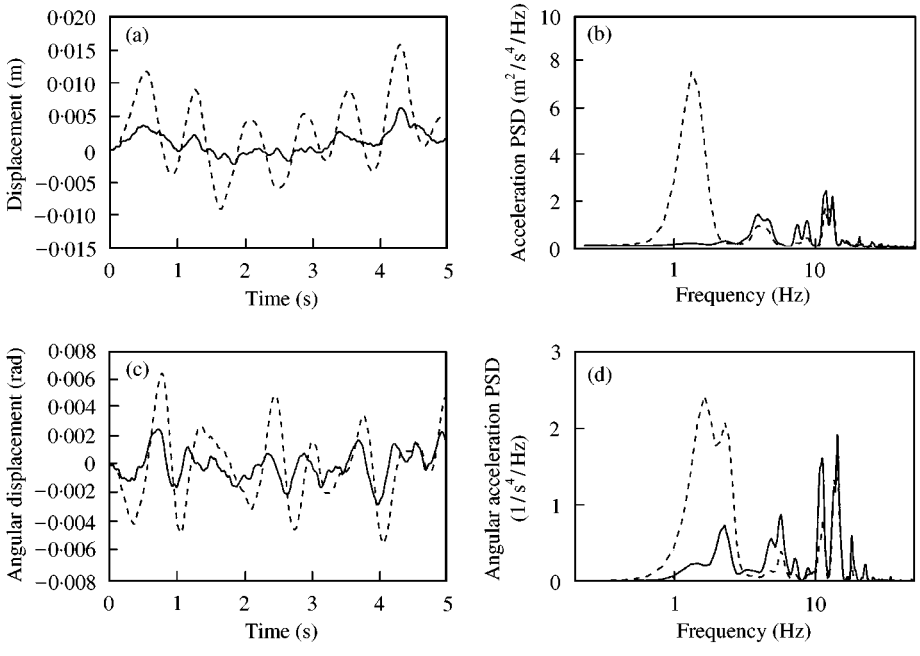

Figure 7. Random responses of the semi-active suspension with the orifice-type ER dampers. (a) Vertical displacement; (b) vertical acceleration PSD; (c) pitch angular displacement; (d) pitch angular acceleration PSD: - - -, 0·0 kV/mm; ——, optimal control.

Here W_m is white noise with intensity $2\sigma^2\rho V$, ρ is the road roughness parameter, and σ^2 is the covariance of road irregularity. In random excitation, the values of road irregularity are chosen assuming that the vehicle travels on the paved road with the constant velocity of 72 km/h (= 20 m/s). The values of $\rho = 0{\cdot}45\ \mathrm{m}^{-1}$ and $\sigma^2 = 300\ \mathrm{mm}^2$ are chosen in the sense of the paved road condition. Figure 7 presents time and frequency responses of the semi-active suspension system subjected to random excitation. It is clearly observed that both the vertical displacement and pitch angular displacement are substantially reduced by applying the optimal controller. The frequency responses are obtained from power spectral density (PSD) for the vertical acceleration of the sprung mass and the pitch angular acceleration of the body. As expected, power spectral densities are also substantially reduced in the neighborhood of body resonance (1–3 Hz). This result directly implies the significant improvement of the ride comfort quality of the vehicle. However, in the frequency range between body resonance and wheel resonance, the sprung mass acceleration is worse than uncontrolled case. This is caused by the dynamic characteristic of the adopted optimal controller. Since there is no acceleration component in the state variables of the optimal controller, the controller attenuates the vehicle motion with only displacement and velocity.

5. CONCLUSIONS

In this work, a new type of electro-rheological (ER) fluid damper, which can produce a relatively high damping force with low level of field-dependent yield stress of ER fluids, was proposed and applied to a semi-active suspension system of a small-sized passenger vehicle. After manufacturing the proposed ER damper, field-dependent damping force

characteristics were experimentally evaluated. It has been shown by using optimal controller that the semi-active suspension system installed with the proposed ER damper can improve ride quality of the vehicle demonstrating the vibration control capabiltiy under bump and random profiles.

It is finally remarked that comparative work between the proposed ER suspension and conventional passive (or semi-active) suspension, the design of robust controllers to attenuate wheel resonance, and the field test on real roads should be undertaken as further studies.

REFERENCES

1. N. K. PETEK 1992 *SAE Technical Paper Series* **920275**. An electronically controlled shock absorber by electro-rheological fluid.
2. M. NAKANO 1995 *Proceedings of the* 5*th International Conference on ER Fluid, MR Suspensions and Associated Technology*, 645. A novel semi-active control of automotive suspension using an electrorheological shock absorber.
3. G. M. KAMATH, M. K. HURT AND N. M. WERELY 1996 *Smart Materials and Structures* **5**, 576. Analysis and testing of Bingham plastic behavior on semi-active electrorheological fluid dampers.
4. R. GORDANINEJAD, A. RAY AND H. WANG 1997 *Journal of Vibration and Acoustics* **119**, 527. Control of forced vibration using multi-electrode electro-rheological fluid dampers.
5. S. B. CHOI, Y. T. CHOI, E. G. CHANG, S. J. HAN AND C. S. KIM 1998 *Mechatronics* **8**, 143. Control characteristics of a continuously variable ER damper.